

Measurements of Absolute Branching Fractions of $D^0 \rightarrow K_L^0 \phi, K_L^0 \eta, K_L^0 \omega,$ and $K_L^0 \eta'$

M. Ablikim¹, M. N. Achasov^{10,c}, P. Adlarson⁶⁷, S. Ahmed¹⁵, M. Albrecht⁴, R. Aliberti²⁸, A. Amoroso^{66A,66C}, M. R. An³², Q. An^{63,49}, X. H. Bai⁵⁷, Y. Bai⁴⁸, O. Bakina²⁹, R. Baldini Ferroli^{23A}, I. Balossino^{24A}, Y. Ban^{38,k}, K. Begzsuren²⁶, N. Berger²⁸, M. Bertani^{23A}, D. Bettoni^{24A}, F. Bianchi^{66A,66C}, J. Bloms⁶⁰, A. Bortone^{66A,66C}, I. Boyko²⁹, R. A. Briere⁵, H. Cai⁶⁸, X. Cai^{1,49}, A. Calcaterra^{23A}, G. F. Cao^{1,54}, N. Cao^{1,54}, S. A. Cetin^{53A}, J. F. Chang^{1,49}, W. L. Chang^{1,54}, G. Chelkov^{29,b}, D. Y. Chen⁶, G. Chen¹, H. S. Chen^{1,54}, M. L. Chen^{1,49}, S. J. Chen³⁵, X. R. Chen²⁵, Y. B. Chen^{1,49}, Z. J. Chen^{20,l}, W. S. Cheng^{66C}, G. Cibinetto^{24A}, F. Cossio^{66C}, X. F. Cui³⁶, H. L. Dai^{1,49}, X. C. Dai^{1,54}, A. Dbeysy¹⁵, R. E. de Boer⁴, D. Dedovich²⁹, Z. Y. Deng¹, A. Denig²⁸, I. Denysenko²⁹, M. Destefanis^{66A,66C}, F. De Mori^{66A,66C}, Y. Ding³³, C. Dong³⁶, J. Dong^{1,49}, L. Y. Dong^{1,54}, M. Y. Dong^{1,49,54}, X. Dong⁶⁸, S. X. Du⁷¹, Y. L. Fan⁶⁸, J. Fang^{1,49}, S. S. Fang^{1,54}, Y. Fang¹, R. Farinelli^{24A}, L. Fava^{66B,66C}, F. Feldbauer⁴, G. Felici^{23A}, C. Q. Feng^{63,49}, J. H. Feng⁵⁰, M. Fritsch⁴, C. D. Fu¹, Y. Gao^{63,49}, Y. Gao^{38,k}, Y. Gao⁶⁴, Y. G. Gao⁶, I. Garzia^{24A,24B}, P. T. Ge⁶⁸, C. Geng⁵⁰, E. M. Gersabeck⁵⁸, A. Gilman⁶¹, K. Goetzen¹¹, L. Gong³³, W. X. Gong^{1,49}, W. Gradl²⁸, M. Greco^{66A,66C}, L. M. Gu³⁵, M. H. Gu^{1,49}, S. Gu², Y. T. Gu¹³, C. Y. Guan^{1,54}, A. Q. Guo²², L. B. Guo³⁴, R. P. Guo⁴⁰, Y. P. Guo^{9,h}, A. Guskov^{29,b}, T. T. Han⁴¹, W. Y. Han³², X. Q. Hao¹⁶, F. A. Harris⁵⁶, N. Hüsken^{22,28}, K. L. He^{1,54}, F. H. Heinsius⁴, C. H. Heinz²⁸, T. Held⁴, Y. K. Heng^{1,49,54}, C. Herold⁵¹, M. Himmelreich^{11,f}, T. Holtmann⁴, G. Y. Hou^{1,54}, Y. R. Hou⁵⁴, Z. L. Hou¹, H. M. Hu^{1,54}, J. F. Hu^{47,m}, T. Hu^{1,49,54}, Y. Hu¹, G. S. Huang^{63,49}, L. Q. Huang⁶⁴, X. T. Huang⁴¹, Y. P. Huang¹, Z. Huang^{38,k}, T. Hussain⁶⁵, W. Ikegami Andersson⁶⁷, W. Imoehl²², M. Irshad^{63,49}, S. Jaeger⁴, S. Janchiv^{26,j}, Q. Ji¹, Q. P. Ji¹⁶, X. B. Ji^{1,54}, X. L. Ji^{1,49}, Y. Y. Ji⁴¹, H. B. Jiang⁴¹, X. S. Jiang^{1,49,54}, J. B. Jiao⁴¹, Z. Jiao¹⁸, S. Jin³⁵, Y. Jin⁵⁷, M. Q. Jing^{1,54}, T. Johansson⁶⁷, N. Kalantar-Nayestanaki⁵⁵, X. S. Kang³³, R. Kappert⁵⁵, M. Kavatsyuk⁵⁵, B. C. Ke^{43,1}, I. K. Keshk⁴, A. Khoukaz⁶⁰, P. Kiese²⁸, R. Kiuchi¹, R. Kliemt¹¹, L. Koch³⁰, O. B. Kolcu^{53A,e}, B. Kopf⁴, M. Kuemmel⁴, M. Kuessner⁴, A. Kupsc⁶⁷, M. G. Kurth^{1,54}, W. Kühn³⁰, J. J. Lane⁵⁸, J. S. Lange³⁰, P. Larin¹⁵, A. Lavanaia²¹, L. Lavezzi^{66A,66C}, Z. H. Lei^{63,49}, H. Leithoff²⁸, M. Lellmann²⁸, T. Lenz²⁸, C. Li³⁹, C. H. Li³², Cheng Li^{63,49}, D. M. Li⁷¹, F. Li^{1,49}, G. Li¹, H. Li^{63,49}, H. Li⁴³, H. B. Li^{1,54}, H. J. Li¹⁶, J. L. Li⁴¹, J. Q. Li⁴, J. S. Li⁵⁰, Ke Li¹, L. K. Li¹, Lei Li³, P. R. Li^{31,n,o}, S. Y. Li⁵², W. D. Li^{1,54}, W. G. Li¹, X. H. Li^{63,49}, X. L. Li⁴¹, Xiaoyu Li^{1,54}, Z. Y. Li⁵⁰, H. Liang^{1,54}, H. Liang^{63,49}, H. Liang²⁷, Y. F. Liang⁴⁵, Y. T. Liang²⁵, G. R. Liao¹², L. Z. Liao^{1,54}, J. Libby²¹, C. X. Lin⁵⁰, B. J. Liu¹, C. X. Liu¹, D. Liu^{15,63}, F. H. Liu⁴⁴, Fang Liu¹, Feng Liu⁶, H. B. Liu¹³, H. M. Liu^{1,54}, Huanhuan Liu¹, Huihui Liu¹⁷, J. B. Liu^{63,49}, J. L. Liu⁶⁴, J. Y. Liu^{1,54}, K. Liu¹, K. Y. Liu³³, L. Liu^{63,49}, M. H. Liu^{9,h}, P. L. Liu¹, Q. Liu⁵⁴, Q. Liu⁶⁸, S. B. Liu^{63,49}, Shuai Liu⁴⁶, T. Liu^{1,54}, W. M. Liu^{63,49}, X. Liu^{31,n,o}, Y. Liu^{31,n,o}, Y. B. Liu³⁶, Z. A. Liu^{1,49,54}, Z. Q. Liu⁴¹, X. C. Lou^{1,49,54}, F. X. Lu⁵⁰, H. J. Lu¹⁸, J. D. Lu^{1,54}, J. G. Lu^{1,49}, X. L. Lu¹, Y. Lu¹, Y. P. Lu^{1,49}, C. L. Luo³⁴, M. X. Luo⁷⁰, P. W. Luo⁵⁰, T. Luo^{9,h}, X. L. Luo^{1,49}, X. R. Lyu⁵⁴, F. C. Ma³³, H. L. Ma¹, L. L. Ma⁴¹, M. M. Ma^{1,54}, Q. M. Ma¹, R. Q. Ma^{1,54}, R. T. Ma⁵⁴, X. X. Ma^{1,54}, X. Y. Ma^{1,49}, F. E. Maas¹⁵, M. Maggiora^{66A,66C}, S. Maldaner⁴, S. Malde⁶¹, Q. A. Malik⁶⁵, A. Mangoni^{23B}, Y. J. Mao^{38,k}, Z. P. Mao¹, S. Marcello^{66A,66C}, Z. X. Meng⁵⁷, J. G. Messchendorp⁵⁵, G. Mezzadri^{24A}, T. J. Min³⁵, R. E. Mitchell²², X. H. Mo^{1,49,54}, Y. J. Mo⁶, N. Yu. Muchnoi^{10,c}, H. Muramatsu⁵⁹, S. Nakhoul^{11,f}, Y. Nefedov²⁹, F. Nerling^{11,f}, I. B. Nikolaev^{10,c}, Z. Ning^{1,49}, S. Nisar^{8,i}, S. L. Olsen⁵⁴, Q. Ouyang^{1,49,54}, S. Pacetti^{23B,23C}, X. Pan^{9,h}, Y. Pan⁵⁸, A. Pathak¹, P. Patteri^{23A}, M. Pelizaeus⁴, H. P. Peng^{63,49}, K. Peters^{11,f}, J. Pettersson⁶⁷, J. L. Ping³⁴, R. G. Ping^{1,54}, R. Poling⁵⁹, V. Prasad^{63,49}, H. Qi^{63,49}, H. R. Qi⁵², K. H. Qi²⁵, M. Qi³⁵, T. Y. Qi⁹, S. Qian^{1,49}, W. B. Qian⁵⁴, Z. Qian⁵⁰, C. F. Qiao⁵⁴, L. Q. Qin¹², X. P. Qin⁹, X. S. Qin⁴¹, Z. H. Qin^{1,49}, J. F. Qiu¹, S. Q. Qu³⁶, K. H. Rashid⁶⁵, K. Ravindran²¹, C. F. Redmer²⁸, A. Rivetti^{66C}, V. Rodin⁵⁵, M. Rolo^{66C}, G. Rong^{1,54}, Ch. Rosner¹⁵, M. Rump⁶⁰, H. S. Sang⁶³, A. Sarantsev^{29,d}, Y. Schelhaas²⁸, C. Schnier⁴, K. Schoenning⁶⁷, M. Scodreggio^{24A,24B}, D. C. Shan⁴⁶, W. Shan¹⁹, X. Y. Shan^{63,49}, J. F. Shangguan⁴⁶, M. Shao^{63,49}, C. P. Shen⁹, H. F. Shen^{1,54}, P. X. Shen³⁶, X. Y. Shen^{1,54}, H. C. Shi^{63,49}, R. S. Shi^{1,54}, X. Shi^{1,49}, X. D. Shi^{63,49}, J. J. Song⁴¹, W. M. Song^{27,1}, Y. X. Song^{38,k}, S. Sosio^{66A,66C}, S. Spataro^{66A,66C}, K. X. Su⁶⁸, P. P. Su⁴⁶, F. F. Sui⁴¹, G. X. Sun¹, H. K. Sun¹, J. F. Sun¹⁶, L. Sun⁶⁸, S. S. Sun^{1,54}, T. Sun^{1,54}, W. Y. Sun²⁷, W. Y. Sun³⁴, X. Sun^{20,l}, Y. J. Sun^{63,49}, Y. K. Sun^{63,49}, Y. Z. Sun¹, Z. T. Sun¹, Y. H. Tan⁶⁸, Y. X. Tan^{63,49}, C. J. Tang⁴⁵, G. Y. Tang¹, J. Tang⁵⁰, J. X. Teng^{63,49}, V. Thoren⁶⁷, W. H. Tian⁴³, Y. T. Tian²⁵, I. Uman^{53B}, B. Wang¹, C. W. Wang³⁵, D. Y. Wang^{38,k}, H. J. Wang^{31,n,o}, H. P. Wang^{1,54}, K. Wang^{1,49}, L. L. Wang¹, M. Wang⁴¹, M. Z. Wang^{38,k}, Meng Wang^{1,54}, W. Wang⁵⁰, W. H. Wang⁶⁸, W. P. Wang^{63,49}, X. Wang^{38,k}, X. F. Wang^{31,n,o}, X. L. Wang^{9,h}, Y. Wang⁵⁰, Y. Wang^{63,49}, Y. D. Wang³⁷, Y. F. Wang^{1,49,54}, Y. Q. Wang¹, Y. Y. Wang^{31,n,o}, Z. Wang^{1,49}, Z. Y. Wang¹, Ziyi Wang⁵⁴,

Zongyuan Wang^{1,54}, D. H. Wei¹², F. Weidner⁶⁰, S. P. Wen¹, D. J. White⁵⁸, U. Wiedner⁴, G. Wilkinson⁶¹, M. Wolke⁶⁷, L. Wollenberg⁴, J. F. Wu^{1,54}, L. H. Wu¹, L. J. Wu^{1,54}, X. Wu^{9,h}, Z. Wu^{1,49}, L. Xia^{63,49}, H. Xiao^{9,h}, S. Y. Xiao¹, Z. J. Xiao³⁴, X. H. Xie^{38,k}, Y. G. Xie^{1,49}, Y. H. Xie⁶, T. Y. Xing^{1,54}, G. F. Xu¹, Q. J. Xu¹⁴, W. Xu^{1,54}, X. P. Xu⁴⁶, Y. C. Xu⁵⁴, F. Yan^{9,h}, L. Yan^{9,h}, W. B. Yan^{63,49}, W. C. Yan⁷¹, Xu Yan⁴⁶, H. J. Yang^{42,g}, H. X. Yang¹, L. Yang⁴³, S. L. Yang⁵⁴, Y. X. Yang¹², Yifan Yang^{1,54}, Zhi Yang²⁵, M. Ye^{1,49}, M. H. Ye⁷, J. H. Yin¹, Z. Y. You⁵⁰, B. X. Yu^{1,49,54}, C. X. Yu³⁶, G. Yu^{1,54}, J. S. Yu^{20,l}, T. Yu⁶⁴, C. Z. Yuan^{1,54}, L. Yuan², X. Q. Yuan^{38,k}, Y. Yuan¹, Z. Y. Yuan⁵⁰, C. X. Yue³², A. Yuncu^{53A,a}, A. A. Zafar⁶⁵, X. Zeng⁶, Y. Zeng^{20,l}, A. Q. Zhang¹, B. X. Zhang¹, Guangyi Zhang¹⁶, H. Zhang⁶³, H. H. Zhang²⁷, H. H. Zhang⁵⁰, H. Y. Zhang^{1,49}, J. J. Zhang⁴³, J. L. Zhang⁶⁹, J. Q. Zhang³⁴, J. W. Zhang^{1,49,54}, J. Y. Zhang¹, J. Z. Zhang^{1,54}, Jianyu Zhang^{1,54}, Jiawei Zhang^{1,54}, L. M. Zhang⁵², L. Q. Zhang⁵⁰, Lei Zhang³⁵, S. Zhang⁵⁰, S. F. Zhang³⁵, Shulei Zhang^{20,l}, X. D. Zhang³⁷, X. Y. Zhang⁴¹, Y. Zhang⁶¹, Y. H. Zhang^{1,49}, Y. T. Zhang^{63,49}, Yan Zhang^{63,49}, Yao Zhang¹, Yi Zhang^{9,h}, Z. H. Zhang⁶, Z. Y. Zhang⁶⁸, G. Zhao¹, J. Zhao³², J. Y. Zhao^{1,54}, J. Z. Zhao^{1,49}, Lei Zhao^{63,49}, Ling Zhao¹, M. G. Zhao³⁶, Q. Zhao¹, S. J. Zhao⁷¹, Y. B. Zhao^{1,49}, Y. X. Zhao²⁵, Z. G. Zhao^{63,49}, A. Zhemchugov^{29,b}, B. Zheng⁶⁴, J. P. Zheng^{1,49}, Y. Zheng^{38,k}, Y. H. Zheng⁵⁴, B. Zhong³⁴, C. Zhong⁶⁴, L. P. Zhou^{1,54}, Q. Zhou^{1,54}, X. Zhou⁶⁸, X. K. Zhou⁵⁴, X. R. Zhou^{63,49}, X. Y. Zhou³², A. N. Zhu^{1,54}, J. Zhu³⁶, K. Zhu¹, K. J. Zhu^{1,49,54}, S. H. Zhu⁶², T. J. Zhu⁶⁹, W. J. Zhu^{9,h}, W. J. Zhu³⁶, Y. C. Zhu^{63,49}, Z. A. Zhu^{1,54}, B. S. Zou¹, J. H. Zou¹

(BESIII Collaboration)

¹ *Institute of High Energy Physics, Beijing 100049, People's Republic of China*

² *Beihang University, Beijing 100191, People's Republic of China*

³ *Beijing Institute of Petrochemical Technology, Beijing 102617, People's Republic of China*

⁴ *Bochum Ruhr-University, D-44780 Bochum, Germany*

⁵ *Carnegie Mellon University, Pittsburgh, Pennsylvania 15213, USA*

⁶ *Central China Normal University, Wuhan 430079, People's Republic of China*

⁷ *China Center of Advanced Science and Technology, Beijing 100190, People's Republic of China*

⁸ *COMSATS University Islamabad, Lahore Campus, Defence Road, Off Raiwind Road, 54000 Lahore, Pakistan*

⁹ *Fudan University, Shanghai 200443, People's Republic of China*

¹⁰ *G.I. Budker Institute of Nuclear Physics SB RAS (BINP), Novosibirsk 630090, Russia*

¹¹ *GSI Helmholtzcentre for Heavy Ion Research GmbH, D-64291 Darmstadt, Germany*

¹² *Guangxi Normal University, Guilin 541004, People's Republic of China*

¹³ *Guangxi University, Nanning 530004, People's Republic of China*

¹⁴ *Hangzhou Normal University, Hangzhou 310036, People's Republic of China*

¹⁵ *Helmholtz Institute Mainz, Staudinger Weg 18, D-55099 Mainz, Germany*

¹⁶ *Henan Normal University, Xinxiang 453007, People's Republic of China*

¹⁷ *Henan University of Science and Technology, Luoyang 471003, People's Republic of China*

¹⁸ *Huangshan College, Huangshan 245000, People's Republic of China*

¹⁹ *Hunan Normal University, Changsha 410081, People's Republic of China*

²⁰ *Hunan University, Changsha 410082, People's Republic of China*

²¹ *Indian Institute of Technology Madras, Chennai 600036, India*

²² *Indiana University, Bloomington, Indiana 47405, USA*

²³ *INFN Laboratori Nazionali di Frascati, (A)INFN Laboratori Nazionali di Frascati, I-00044, Frascati, Italy; (B)INFN Sezione di Perugia, I-06100, Perugia, Italy; (C)University of Perugia, I-06100, Perugia, Italy*

²⁴ *INFN Sezione di Ferrara, (A)INFN Sezione di Ferrara, I-44122, Ferrara, Italy; (B)University of Ferrara, I-44122, Ferrara, Italy*

²⁵ *Institute of Modern Physics, Lanzhou 730000, People's Republic of China*

²⁶ *Institute of Physics and Technology, Peace Ave. 54B, Ulaanbaatar 13330, Mongolia*

²⁷ *Jilin University, Changchun 130012, People's Republic of China*

²⁸ *Johannes Gutenberg University of Mainz, Johann-Joachim-Becher-Weg 45, D-55099 Mainz, Germany*

²⁹ *Joint Institute for Nuclear Research, 141980 Dubna, Moscow region, Russia*

³⁰ *Justus-Liebig-Universität Giessen, II. Physikalisches Institut, Heinrich-Buff-Ring 16, D-35392 Giessen, Germany*

³¹ *Lanzhou University, Lanzhou 730000, People's Republic of China*

³² *Liaoning Normal University, Dalian 116029, People's Republic of China*

- ³³ Liaoning University, Shenyang 110036, People's Republic of China
- ³⁴ Nanjing Normal University, Nanjing 210023, People's Republic of China
- ³⁵ Nanjing University, Nanjing 210093, People's Republic of China
- ³⁶ Nankai University, Tianjin 300071, People's Republic of China
- ³⁷ North China Electric Power University, Beijing 102206, People's Republic of China
- ³⁸ Peking University, Beijing 100871, People's Republic of China
- ³⁹ Qufu Normal University, Qufu 273165, People's Republic of China
- ⁴⁰ Shandong Normal University, Jinan 250014, People's Republic of China
- ⁴¹ Shandong University, Jinan 250100, People's Republic of China
- ⁴² Shanghai Jiao Tong University, Shanghai 200240, People's Republic of China
- ⁴³ Shanxi Normal University, Linfen 041004, People's Republic of China
- ⁴⁴ Shanxi University, Taiyuan 030006, People's Republic of China
- ⁴⁵ Sichuan University, Chengdu 610064, People's Republic of China
- ⁴⁶ Soochow University, Suzhou 215006, People's Republic of China
- ⁴⁷ South China Normal University, Guangzhou 510006, People's Republic of China
- ⁴⁸ Southeast University, Nanjing 211100, People's Republic of China
- ⁴⁹ State Key Laboratory of Particle Detection and Electronics, Beijing 100049, Hefei 230026, People's Republic of China
- ⁵⁰ Sun Yat-Sen University, Guangzhou 510275, People's Republic of China
- ⁵¹ Suranaree University of Technology, University Avenue 111, Nakhon Ratchasima 30000, Thailand
- ⁵² Tsinghua University, Beijing 100084, People's Republic of China
- ⁵³ Turkish Accelerator Center Particle Factory Group, (A)Istanbul Bilgi University, 34060 Eyup, Istanbul, Turkey; (B)Near East University, Nicosia, North Cyprus, Mersin 10, Turkey
- ⁵⁴ University of Chinese Academy of Sciences, Beijing 100049, People's Republic of China
- ⁵⁵ University of Groningen, NL-9747 AA Groningen, The Netherlands
- ⁵⁶ University of Hawaii, Honolulu, Hawaii 96822, USA
- ⁵⁷ University of Jinan, Jinan 250022, People's Republic of China
- ⁵⁸ University of Manchester, Oxford Road, Manchester, M13 9PL, United Kingdom
- ⁵⁹ University of Minnesota, Minneapolis, Minnesota 55455, USA
- ⁶⁰ University of Muenster, Wilhelm-Klemm-Str. 9, 48149 Muenster, Germany
- ⁶¹ University of Oxford, Keble Rd, Oxford, UK OX13RH
- ⁶² University of Science and Technology Liaoning, Anshan 114051, People's Republic of China
- ⁶³ University of Science and Technology of China, Hefei 230026, People's Republic of China
- ⁶⁴ University of South China, Hengyang 421001, People's Republic of China
- ⁶⁵ University of the Punjab, Lahore-54590, Pakistan
- ⁶⁶ University of Turin and INFN, (A)University of Turin, I-10125, Turin, Italy; (B)University of Eastern Piedmont, I-15121, Alessandria, Italy; (C)INFN, I-10125, Turin, Italy
- ⁶⁷ Uppsala University, Box 516, SE-75120 Uppsala, Sweden
- ⁶⁸ Wuhan University, Wuhan 430072, People's Republic of China
- ⁶⁹ Xinyang Normal University, Xinyang 464000, People's Republic of China
- ⁷⁰ Zhejiang University, Hangzhou 310027, People's Republic of China
- ⁷¹ Zhengzhou University, Zhengzhou 450001, People's Republic of China
- ^a Also at Bogazici University, 34342 Istanbul, Turkey
- ^b Also at the Moscow Institute of Physics and Technology, Moscow 141700, Russia
- ^c Also at the Novosibirsk State University, Novosibirsk, 630090, Russia
- ^d Also at the NRC "Kurchatov Institute", PNPI, 188300, Gatchina, Russia
- ^e Also at Istanbul Arel University, 34295 Istanbul, Turkey
- ^f Also at Goethe University Frankfurt, 60323 Frankfurt am Main, Germany
- ⁹ Also at Key Laboratory for Particle Physics, Astrophysics and Cosmology, Ministry of Education; Shanghai Key Laboratory for Particle Physics and Cosmology; Institute of Nuclear and Particle Physics, Shanghai 200240, People's Republic of China

^h Also at Key Laboratory of Nuclear Physics and Ion-beam Application (MOE) and Institute of Modern Physics, Fudan University, Shanghai 200443, People's Republic of China

ⁱ Also at Harvard University, Department of Physics, Cambridge, MA, 02138, USA

^j Currently at: Institute of Physics and Technology, Peace Ave.54B, Ulaanbaatar 13330, Mongolia

^k Also at State Key Laboratory of Nuclear Physics and Technology,

Peking University, Beijing 100871, People's Republic of China

^l School of Physics and Electronics, Hunan University, Changsha 410082, China

^m Also at Guangdong Provincial Key Laboratory of Nuclear Science, Institute of Quantum Matter, South China Normal University, Guangzhou 510006, China

ⁿ Frontier Science Center for Rare Isotopes, Lanzhou University, Lanzhou 730000, People's Republic of China

^o Lanzhou Center for Theoretical Physics, Lanzhou University, Lanzhou 730000, People's Republic of China

We report the first measurements of the absolute branching fractions of $D^0 \rightarrow K_L^0 \phi$, $D^0 \rightarrow K_L^0 \eta$, $D^0 \rightarrow K_L^0 \omega$, and $D^0 \rightarrow K_L^0 \eta'$, by analyzing 2.93 fb^{-1} of e^+e^- collision data taken at a center-of-mass energy of 3.773 GeV with the BESIII detector. Taking the world averages of the branching fractions of $D^0 \rightarrow K_S^0 \phi$, $D^0 \rightarrow K_S^0 \eta$, $D^0 \rightarrow K_S^0 \omega$, and $D^0 \rightarrow K_S^0 \eta'$, the K_S^0 - K_L^0 asymmetries $\mathcal{R}(D^0, X)$ in these decay modes are obtained. The CP asymmetries in these decays are also determined. No significant CP violation is observed.

Hadronic decays of charmed mesons offer an ideal testbed to investigate strong and weak interactions. Remarkable progress in studies of hadronic D decays involving K^\pm and K_S^0 has been achieved to date. However, experimental knowledge of hadronic D decays involving a K_L^0 is still very poor [1] mainly due to the difficulty in K_L^0 reconstruction. It is often assumed (or taken as a good approximation) that the branching fractions (BFs) of D decays into hadronic final states containing K_L^0 meson(s) are equal to those for the corresponding final states with K_S^0 meson(s). However, as clarified in Refs. [2–7], the interference between Cabibbo-Favored (CF) and Doubly-Cabibbo-Suppressed (DCS) amplitudes can lead to a significant asymmetry between the BFs of $D^0 \rightarrow K_S^0 X$ and $D^0 \rightarrow K_L^0 X$ ($X = \pi^0, \eta, \eta', \omega, \rho^0$, and ϕ),

$$\begin{aligned} \mathcal{R}(D^0, X) &= \frac{\mathcal{B}(D^0 \rightarrow K_S^0 X) - \mathcal{B}(D^0 \rightarrow K_L^0 X)}{\mathcal{B}(D^0 \rightarrow K_S^0 X) + \mathcal{B}(D^0 \rightarrow K_L^0 X)} \\ &= -2r \cos \delta + y_D, \end{aligned} \quad (1)$$

where r and δ are the relative strength and phase between the DCS and CF amplitudes, respectively, and y_D is the D^0 - \bar{D}^0 mixing parameter [8]. One has $\mathcal{R}(D^0, P) = 2 \tan^2 \theta_C (+y_D) = 0.113 \pm 0.001$ for $P = \pi^0, \eta$, or η' naively [2–6], where θ_C is the Cabibbo mixing angle [9]. Using the factorization-assisted topological (FAT) amplitude approach and assuming $E_P = E_V$, Ref. [6] stated that the $\mathcal{R}(D^0, V)$ for $V = \rho, \omega$, or ϕ can also be simplified as $2 \tan^2 \theta_C + y_D = 0.113 \pm 0.001$, where E_P and E_V are the W -exchange amplitudes for $D \rightarrow PP$ and $D \rightarrow VP$ decays, respectively. Here, P and V denote pseudoscalar and vector mesons, respectively. It is independent of X because the ratio of DCS and CF amplitudes only depends on the Cabibbo-Kobayashi-Maskawa (CKM) matrix elements. The large asymmetry for $\mathcal{R}(D^0, \pi^0)$ has been confirmed by a previous measurement of the CLEO experiment [10]. Measurements

of the BFs of $D^0 \rightarrow K_L^0 \phi$, $D^0 \rightarrow K_L^0 \eta$, $D^0 \rightarrow K_L^0 \omega$, and $D^0 \rightarrow K_L^0 \eta'$ are crucial to test theoretical calculations and help understand the CKM mechanism. Study of the K_S^0 - K_L^0 asymmetry, $\mathcal{R}(D, X)$ is also important to improve the understanding of quark U-spin [11, 12] and SU(3)-flavor symmetry breaking effects and can benefit theoretical predictions of CP violation in D decays [13–21]. These decays are all $CP+$ eigenstates and can be used to extract the strong phase differences of neutral D decays [22, 23].

Studies of CP violation of the weak decays of D mesons are important for exploring physics within and beyond the Standard Model. The size of CP violation in various D decays is predicted to be in the order of 10^{-3} [19, 24–29]. In 2019, LHCb reported the first observation of CP violation in neutral D decays [30]. Currently, the knowledge of CP violation in the charm sector is still limited and further measurements are highly desirable.

This paper reports the first measurements of the BFs of $D^0 \rightarrow K_L^0 \phi$, $D^0 \rightarrow K_L^0 \eta$, $D^0 \rightarrow K_L^0 \omega$, and $D^0 \rightarrow K_L^0 \eta'$ as well as the BF asymmetries between $D^0 \rightarrow K_S^0 X$ and $D^0 \rightarrow K_L^0 X$. In addition, the CP asymmetries in these decays are also determined. Throughout this paper, charge conjugate channels are implied, unless noted otherwise.

This analysis is performed with a 2.93 fb^{-1} [31] sample of e^+e^- annihilation data taken at a center-of-mass energy $\sqrt{s} = 3.773 \text{ GeV}$ with the BESIII detector. Details about the design and performance of the BESIII detector are given in Ref. [32]. Simulated samples, produced with the GEANT4-based [33] Monte Carlo (MC) package including the geometric description of the BESIII detector and the detector response, are used to determine the detection efficiency and to estimate background contributions. The simulation includes the beam-energy spread and initial-state radiation in the e^+e^- annihilations mod-

eled with the generator KKMC [34]. An inclusive MC sample, containing the production of $D\bar{D}$ pairs, the non- $D\bar{D}$ decays of the $\psi(3770)$, the initial-state radiation production of the J/ψ and $\psi(3686)$ states, and the continuum processes, is used in this analysis. Known decay modes are modeled with EVTGEN [35] using the BF's taken from the Particle Data Group (PDG) [1] and the remaining unknown decays from the charmonium states are modeled with LUNDCHARM [36]. Final state radiation from charged final-state particles is incorporated using PHOTOS [37].

At $\sqrt{s} = 3.773$ GeV, D^0 and \bar{D}^0 mesons are produced in pairs without accompanying hadrons, and hence the environment is ideal to investigate D^0 decays with the double-tag (DT) method [38]. In this method, the \bar{D}^0 meson, later referred as single-tag (ST), is first reconstructed through the hadronic decays $\bar{D}^0 \rightarrow K^+\pi^-$, $K^+\pi^-\pi^0$, and $K^+\pi^-\pi^-\pi^+$, which have large BF's and small background contamination. If a signal $D^0 \rightarrow K_L^0\phi$, $K_L^0\eta$, $K_L^0\omega$, or $K_L^0\eta'$ decay can be reconstructed in the rest of the event, the event is then considered as a DT event. The BF of the signal decay is determined by

$$\mathcal{B}_{\text{sig}} = N_{\text{DT}} / (N_{\text{ST}}^{\text{tot}} \cdot \epsilon_{\text{sig}}), \quad (2)$$

where $N_{\text{ST}}^{\text{tot}}$ and N_{DT} are the yields of the total ST and DT candidates in data, respectively, and $\epsilon_{\text{sig}} = \sum_i [(\epsilon_{\text{DT}}^i \cdot N_{\text{ST}}^i) / (\epsilon_{\text{ST}}^i \cdot N_{\text{ST}}^{\text{tot}})]$ is the effective signal efficiency of finding the signal decay in the presence of the ST \bar{D}^0 meson, where ϵ_{ST} and ϵ_{DT} are the detection efficiencies of the ST and DT candidates, respectively, and the index i runs over all ST modes.

In the work described in this paper, candidates for K^\pm , π^\pm , γ , and π^0 are selected by using the same selection criteria as in Ref. [39]. The two-body ST mode $\bar{D}^0 \rightarrow K^+\pi^-$ suffers from background contributions from cosmic rays and Bhabha scattering events. These background contributions are rejected by using the same requirements as in Ref. [40]. For the $\bar{D}^0 \rightarrow K^+\pi^-\pi^-\pi^+$ ST mode, the $\bar{D}^0 \rightarrow K_S^0 K^\pm \pi^\mp$ decays are rejected if the mass of any $\pi^+\pi^-$ pair falls within (0.483, 0.513) GeV/ c^2 .

Two kinematic variables, the energy difference $\Delta E \equiv E_{\bar{D}^0} - E_{\text{beam}}$ and the beam-constrained mass $M_{\text{BC}} \equiv \sqrt{E_{\text{beam}}^2/c^4 - |\vec{p}_{\bar{D}^0}|^2/c^2}$ are used to separate the ST \bar{D}^0 mesons from combinatorial backgrounds. Here, E_{beam} is the beam energy and $E_{\bar{D}^0}$ and $\vec{p}_{\bar{D}^0}$ denote the total energy and momentum of the ST \bar{D}^0 candidate in the e^+e^- center-of-mass frame, respectively. If there are multiple combinations in an event, only the combination with the smallest $|\Delta E|$ is accepted. To suppress combinatorial backgrounds, the ΔE of any ST candidate is required to be within (-0.055, 0.040) GeV for $\bar{D}^0 \rightarrow K^+\pi^-\pi^0$ and within (-0.025, 0.025) GeV for $\bar{D}^0 \rightarrow K^+\pi^-$ and $\bar{D}^0 \rightarrow K^+\pi^-\pi^-\pi^+$.

The M_{BC} distributions of the accepted ST \bar{D}^0 candidates are shown in Fig. 1. To extract the yield of ST \bar{D}^0

mesons for each ST mode, a binned maximum-likelihood fit is performed on the corresponding M_{BC} distribution. The signal is modeled by the MC-simulated shape convolved with a double-Gaussian function to take into account the resolution difference between data and MC simulation. In the fits, the Gaussian means and widths are free parameters whose ranges are (0.04, 0.20) MeV/ c^2 and (0.73, 3.19) MeV/ c^2 , respectively. The combinatorial background is described by the ARGUS function [41]. The associated fit results are shown in Fig. 1. The candidates with $M_{\text{BC}} \in (1.859, 1.873)$ GeV/ c^2 are kept for further analyses. Integrating the fitted signal shape in the aforementioned M_{BC} interval gives the yield of the ST \bar{D}^0 mesons for each ST mode. Summing over all ST modes, the total yield of ST \bar{D}^0 mesons is obtained to be $N_{\text{ST}}^{\text{tot}} = 2266311 \pm 1842$.

The $D^0 \rightarrow K_L^0 X$ candidates are reconstructed with charged and photon candidates which have not been used in the ST side. Candidates for ϕ and ω are reconstructed from K^+K^- and $\pi^+\pi^-\pi^0$ combinations with $M_{K^+K^-} \in (1.005, 1.035)$ GeV/ c^2 and $M_{\pi^+\pi^-\pi^0} \in (0.752, 0.812)$ GeV/ c^2 , respectively. Candidates for η are reconstructed from $\gamma\gamma$ pairs with $M_{\gamma\gamma} \in (0.510, 0.570)$ GeV/ c^2 or $\pi^+\pi^-\pi^0$ combinations with $M_{\pi^+\pi^-\pi^0} \in (0.535, 0.560)$ GeV/ c^2 . Candidates for η' are reconstructed from $\pi^+\pi^-\eta$ ($\eta \rightarrow \gamma\gamma$) combinations with $M_{\pi^+\pi^-\eta} \in (0.945, 0.970)$ GeV/ c^2 or $\gamma\rho^0$ ($\rho^0 \rightarrow \pi^+\pi^-$) combinations with $M_{\gamma\rho^0} \in (0.938, 0.978)$ GeV/ c^2 . To improve resolution of $\eta \rightarrow \gamma\gamma$, a mass constrained (1C) fit is performed, constraining the selected $\gamma\gamma$ pair invariant mass to the known η mass [1]. If there are multiple combinations of π^0 or $\eta_{\gamma\gamma}$, the one with the least $\chi_{1\text{C}}^2$ is kept for further analyses. For $\eta' \rightarrow \gamma\rho^0$ ($\rho^0 \rightarrow \pi^+\pi^-$), the $\pi^+\pi^-$ system is required to satisfy $M_{\pi^+\pi^-} \in (0.57, 0.97)$ GeV/ c^2 . For $D^0 \rightarrow K_L^0\eta'_{\gamma\rho^0}$, the background events from $D^0 \rightarrow K_L^0\pi^+\pi^-$ are suppressed by requiring that the recoil mass of the $\pi^+\pi^-$ pair from the signal combined with the ST particles is greater than 0.53 GeV/ c^2 . This requirement suppresses 90% of background events from $D^0 \rightarrow K_L^0\pi^+\pi^-$ at the cost of losing 0.5% of the signal. If there are multiple $\gamma\rho^0$ combinations for $D^0 \rightarrow K_L^0\eta'_{\gamma\rho^0}$, the one with $M_{\gamma\rho^0}$ closest to the known η' mass [1] is kept for further analyses. Throughout this paper, the subscripts of ϕ , η , ω , and η' denote the corresponding reconstruction modes.

To minimize the impact of a K_L^0 shower in electromagnetic calorimeter on an extra π^0 and η vetoes, the opening angle between any remaining photon and the missing momentum is required to be greater than 15° . Events with extra charged tracks, π^0 or $\eta_{\gamma\gamma}$ are rejected to suppress background contributions from $D^0 \rightarrow K_S^0(\rightarrow \pi^+\pi^-)X$, $D^0 \rightarrow K_S^0(\rightarrow \pi^0\pi^0)X$ and $D^0 \rightarrow \eta_{\gamma\gamma}X$, respectively.

To separate signal events from background contributions, the variable $\text{MM}^2 = E_{\text{miss}}^2/c^4 - |\vec{p}_{\text{miss}}|^2/c^2$ is defined, where E_{miss} and \vec{p}_{miss} are the missing energy and

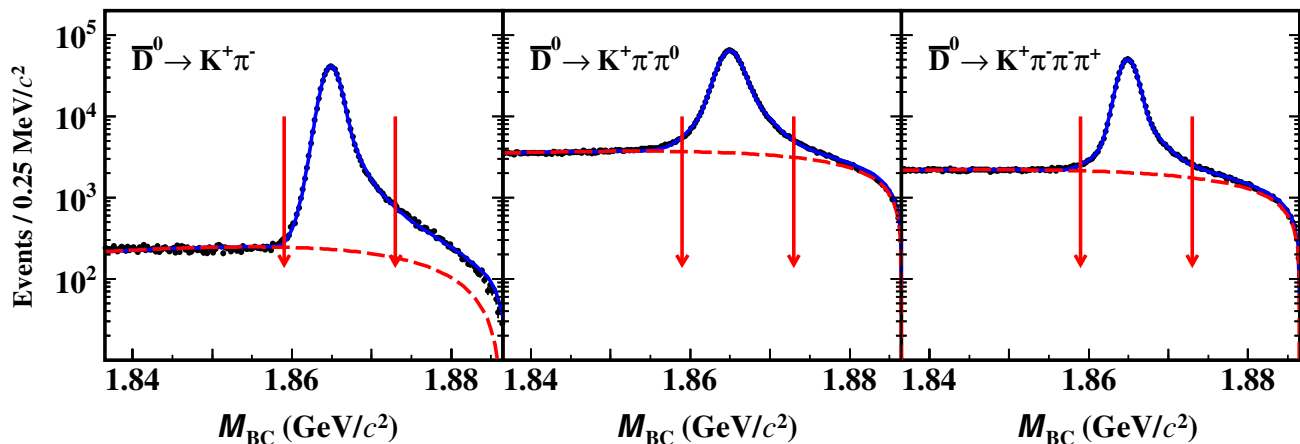


Fig. 1. Fits to the M_{BC} distributions of the ST \bar{D}^0 candidates. Data are shown as dots (error bars are not visible at this scale). The blue solid and red dashed curves are the total fit results and the fitted backgrounds, respectively. Pairs of red arrows show the M_{BC} signal region.

momentum of the DT event in the e^+e^- center-of-mass frame, respectively. They are calculated as $E_{\text{miss}} \equiv E_{D^0} - E_X$ and $\vec{p}_{\text{miss}} \equiv \vec{p}_{D^0} - \vec{p}_X$, where E_{D^0} , \vec{p}_{D^0} , E_X and \vec{p}_X are the measured energy and momentum of the D^0 and X candidates, respectively. The MM^2 resolution is improved by constraining the energy of D^0 to the beam energy and $\vec{p}_{D^0} \equiv -\hat{p}_{D^0} \cdot \sqrt{E_{\text{beam}}^2/c^4 - m_{D^0}^2}$, where \hat{p}_{D^0} is the unit vector in the momentum direction of the ST \bar{D}^0 meson and m_{D^0} is the known \bar{D}^0 mass [1].

The signal yields (N_{sig}) are extracted by fitting the MM^2 distributions of selected events. Background events are divided into four categories. The first (BKGI) contains $D^0 \rightarrow K_S^0(\rightarrow \pi^0\pi^0)X$ events. The second (BKGII) contains $D^0 \rightarrow \eta_{\gamma\gamma}\phi, \eta_{\gamma\gamma}\eta, \eta_{\gamma\gamma}\eta'$ events. The third (BKGIII) is from all the remaining peaking background channels. The fourth (BKGIV) is from combinatorial background components. In the fits, the signal is modeled by the MC-simulated shape convolved with a double-Gaussian function. The means and widths of signal mode dependent Gaussian functions are in the intervals $(-0.58, 1.97) \text{ MeV}^2/c^4$ and $(0.16, 3.70) \text{ MeV}^2/c^4$, respectively. The BKGI and BKGII are described by the corresponding MC-simulated shapes, and their sizes are fixed to the values estimated using the BF's from the PDG [1] and the corresponding misidentification rates. The shape and size of BKGIII are fixed to those obtained from the inclusive MC sample. BKGIV for $D^0 \rightarrow K_L^0\eta'_{\gamma\rho^0}$ is not smooth and is modeled by the MC-simulated shape; it is modeled by a linear function for the other signal decays. Figure 2 shows the results of the fits to the MM^2 distributions of the accepted candidates in data.

There are combinatorial backgrounds in the $\phi \rightarrow K^+K^-$, $\eta \rightarrow \pi^+\pi^-\pi^0$, $\omega \rightarrow \pi^+\pi^-\pi^0$, and $\eta' \rightarrow \pi^+\pi^-\eta$ signal regions, which can form a peak in the

MM^2 distributions. This kind of background is estimated by the corresponding sideband regions, defined as $M_{K^+K^-} \in (0.985, 1.000) \cup (1.045, 1.060) \text{ GeV}/c^2$, $M_{\pi^+\pi^-\pi^0} \in (0.495, 0.515) \cup (0.580, 0.600) \text{ GeV}/c^2$, $M_{\pi^+\pi^-\eta} \in (0.712, 0.732) \cup (0.832, 0.852) \text{ GeV}/c^2$, $M_{\pi^+\pi^-\eta} \in (0.913, 0.938) \cup (0.978, 1.003) \text{ GeV}/c^2$. Their yields (N_{sid}) are obtained from similar fits to individual MM^2 distributions. Table 1 summarizes the fitted yields of N_{sig} and N_{sid} , the normalization factors of background events in the signal and sideband regions (S_{co}), the net signal yield ($N_{\text{net}} = N_{\text{sig}} - N_{\text{sid}} \cdot S_{\text{co}}$), the signal efficiencies (ϵ_{sig}), and the obtained BF's (\mathcal{B}_{sig}).

At $\sqrt{s} = 3.773 \text{ GeV}$, the $D^0\bar{D}^0$ pairs are produced coherently. The measurements of BF's with the DT method are affected by the quantum correlation (QC) effect. Following Ref. [42], this effect is considered as a tag-mode-dependent correction factor, $f_{\text{QC}}^i = \frac{1}{1 - C_f^i \cdot (2F_+^{\text{sig}} - 1)}$, where C_f^i is the strong-phase factor calculated as $C_f^i = \frac{2r_i R_i \cos\delta_f^i}{1 + r_f^2}$, R_i is the coherence factor, δ_f^i is the strong-phase difference between the CF and DCS amplitudes, r_f^i is defined as $r_f^i e^{-i\delta_f^i} \equiv \frac{\langle f | \bar{D}^0 \rangle}{\langle f | D^0 \rangle}$, for the tag mode i ; and F_+^{sig} is the $CP+$ fraction for the signal decay and it equals to 1 for all the studied decays. With necessary parameters quoted from Refs. [43, 44], the f_{QC}^i factors are determined to be 0.898 ± 0.007 , 0.935 ± 0.007 , and 0.972 ± 0.019 for $D \rightarrow K^-\pi^+$, $D \rightarrow K^-\pi^+\pi^0$, and $D \rightarrow K^-\pi^+\pi^+\pi^-$, respectively. All signal decay final states studied are $CP+$ eigenstates. The averaged QC correction factor, which has been weighted by the ST yields in data, is determined to be $f_{\text{QC}} = 0.937 \pm 0.007$. Multiplying the directly-measured BF's by this factor yields the reported BF's. After this correction, the residual uncertainty of f_{QC} will be assigned as a systematic uncertainty. For

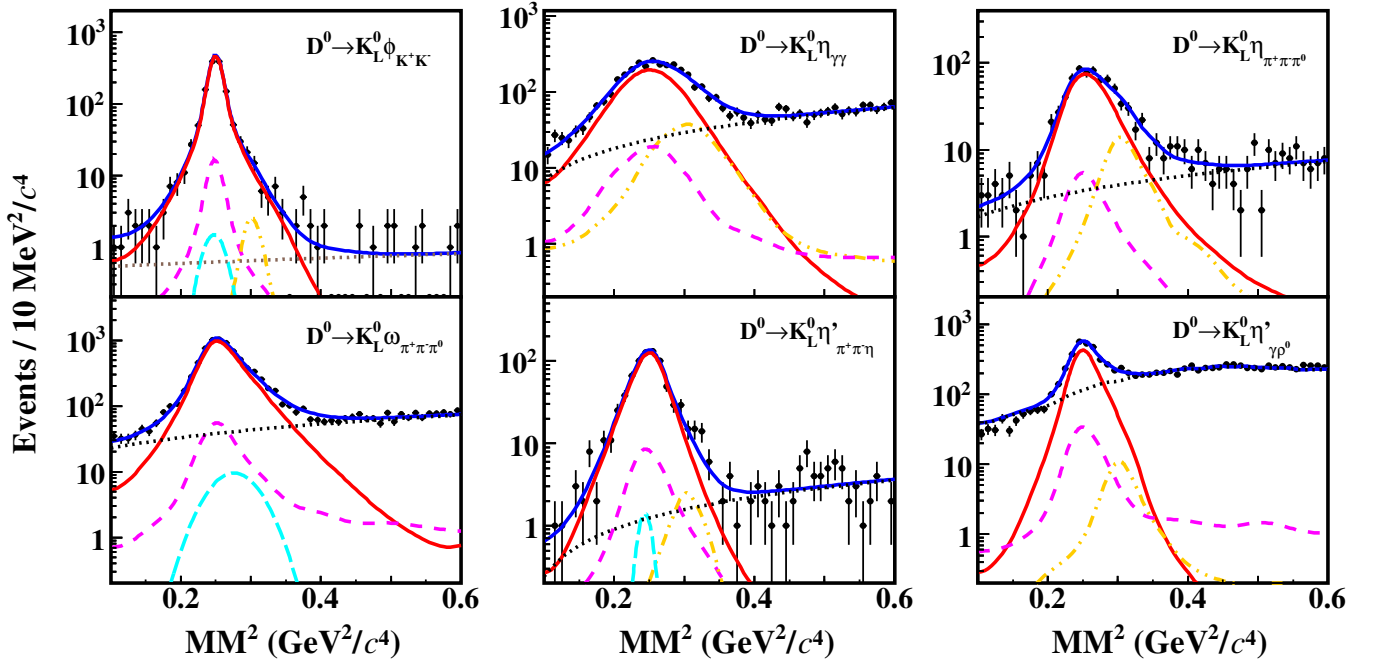


Fig. 2. Fits to the MM^2 distributions of the accepted candidate events. Data are shown as points with error bars. Blue solid curves are the fit result, red solid curves are the signal, pink dashed, yellow long-dashed-dotted, light blue dashed-dotted, and black dotted curves denote BKG I, BKG II, BKG III, and BKG IV, respectively.

$D^0 \rightarrow K_L^0 \eta$ and $D^0 \rightarrow K_L^0 \eta'$, the BF's measured by two different η or η' decay modes have been weighted by the combined statistical and independent uncertainties and the obtained results are shown in Table 1.

In the measurements of the BF's for $D^0 \rightarrow K_L^0 X$ using the DT method, the systematic uncertainties associated with the ST selection are canceled. The major sources of systematic uncertainties related to the measured BF's are described below.

The uncertainty in the total yield of ST \bar{D}^0 mesons has been studied in Ref. [45] and is evaluated as 0.5%. The tracking and particle identification (PID) efficiencies of charged kaons and pions are studied by analyzing DT hadronic $D\bar{D}$ events [46]. The data/MC differences in various momentum intervals are re-weighted by the corresponding momentum distributions of the signal decays. We correct the MC efficiencies to data by signal mode dependent factors of (0.2 – 5.5)%, where the larger difference between data and MC simulation comes from the tracking efficiencies for low momentum K in $D^0 \rightarrow K_L^0 \phi_{K^+K^-}$ decay. The residual systematic uncertainties are (0.2 – 0.6)% for tracking and PID efficiencies per K^\pm or π^\pm .

The systematic uncertainty due to the photon detection in $D^0 \rightarrow K_L^0 \eta'_{\rho^0\gamma}$ decay is 1.0% per photon, as estimated from a $J/\psi \rightarrow \rho^0 \pi^0$ control sample [47]

The systematic uncertainty of π^0 reconstruction has been studied by using the DT events of $\bar{D}^0 \rightarrow K^+ \pi^-$,

$K^+ \pi^- \pi^- \pi^+$ vs. $D^0 \rightarrow K^- \pi^+ \pi^0$ and $K_S^0 \pi^0$ [45]. After correcting the MC efficiencies to agree with data using the momentum-weighted difference (0.5 – 0.6)%, the residual systematic uncertainty, 0.7%, is assigned as the systematic uncertainty in π^0 reconstruction. Due to the limited size of the η sample, the uncertainties of the η reconstruction in $D^0 \rightarrow K_L^0 \eta \gamma \gamma$ and $D^0 \rightarrow K_L^0 \eta'_{\pi^+\pi^-} \eta$ decays are assigned to be 0.5% and 0.7% by referring to the π^0 reconstruction.

The systematic uncertainties due to the mass windows of $\phi_{K^+K^-}$, $\eta_{\pi^+\pi^-\pi^0}$, $\omega_{\pi^+\pi^-\pi^0}$, $\eta'_{\pi^+\pi^-\eta}$, and $\eta'_{\rho^0\gamma}$ candidates are studied using control samples of $D^0 \rightarrow K_S^0 \phi_{K^+K^-}$, $K_S^0 \eta_{\pi^+\pi^-\pi^0}$, $K_S^0 \omega_{\pi^+\pi^-\pi^0}$, $K_S^0 \eta'_{\pi^+\pi^-\eta}$, and $K_S^0 \eta'_{\rho^0\gamma}$, respectively. The relative differences of (0.2 – 0.5)% in the acceptance efficiencies between data and MC simulation are taken as individual systematic uncertainties.

The systematic uncertainty due to requiring no extra charged track, π^0 and η is studied using the control sample of $D^0 \rightarrow K_S^0 \pi^0$. The relative difference in efficiencies between data and MC simulation, 0.8%, is assigned as the systematic uncertainty.

The systematic uncertainties arising from the MM^2 fits are evaluated by varying the signal shape, the background shape, and the size of peaking backgrounds within their uncertainties. The relative changes of various re-measured BF's are added in quadrature and these totals, (0.9 – 2.4)%, are taken as the corresponding sys-

Table 1. The quantities used for BF determinations and the obtained BFs. The signal efficiencies include the BFs for all possible sub-decays and necessary correction factors mentioned later. The listed BFs have been corrected by the QC factor f_{QC} and $\bar{\mathcal{B}}$ denotes the weighted average BFs for $D^0 \rightarrow K_L^0 \eta$ and $D^0 \rightarrow K_L^0 \eta'$. The first and second uncertainties for \mathcal{B} are statistical and systematic, respectively; uncertainties for other variables are statistical only.

Decay	N_{sig}	N_{sid}	S_{co}	N_{net}	$\epsilon_{\text{sig}}(\%)$	$\mathcal{B}_{\text{sig}}(\%)$	$\bar{\mathcal{B}}_{\text{sig}}(\%)$
$D^0 \rightarrow K_L^0 \phi_{K^+K^-}$	1271 ± 39	276 ± 19	1.33 ± 0.17	904 ± 46	9.02 ± 0.10	$0.414 \pm 0.021 \pm 0.010$...
$D^0 \rightarrow K_L^0 \eta_{\gamma\gamma}$	2132 ± 71	2132 ± 71	20.46 ± 0.15	$0.431 \pm 0.014 \pm 0.013$	$0.433 \pm 0.012 \pm 0.010$
$D^0 \rightarrow K_L^0 \eta_{\pi^+\pi^-\pi^0}$	565 ± 29	36 ± 10	0.61 ± 0.10	543 ± 30	5.11 ± 0.07	$0.439 \pm 0.024 \pm 0.015$	
$D^0 \rightarrow K_L^0 \omega_{\pi^+\pi^-\pi^0}$	6692 ± 100	368 ± 39	1.58 ± 0.07	6110 ± 118	21.70 ± 0.18	$1.164 \pm 0.022 \pm 0.028$...
$D^0 \rightarrow K_L^0 \eta'_{\pi^+\pi^-\eta}$	688 ± 29	8 ± 6	0.47 ± 0.08	684 ± 29	3.30 ± 0.10	$0.857 \pm 0.037 \pm 0.022$	$0.809 \pm 0.020 \pm 0.016$
$D^0 \rightarrow K_L^0 \eta'_{\rho^0\gamma}$	2002 ± 61	2002 ± 61	10.55 ± 0.15	$0.785 \pm 0.024 \pm 0.023$	

tematic uncertainties.

The BFs with alternative sideband regions of $M_{K^+K^-}$ and $M_{\pi^+\pi^-\pi^0}$ (± 10 MeV/ c^2 or ± 15 MeV/ c^2) as well as the requirement of $M_{\pi^+\pi^-}^{\text{recoil}}$ (enlarged by 20 MeV/ c^2) are examined. Accounting for correlations, changes in the re-measured BFs are negligible.

To estimate the systematic uncertainties due to the requirement of the opening angle between any remaining shower and the missing momentum of $\bar{D}^0 X$, the BFs are measured using different angle requirements. The maximum deviation of the BFs from (0.9 – 1.6)% is taken as the systematic uncertainty.

The uncertainties of the quoted BFs [1] of $\phi \rightarrow K^+K^-$, $\eta \rightarrow \gamma\gamma$, $\eta \rightarrow \pi^+\pi^-\pi^0$, $\omega \rightarrow \pi^+\pi^-\pi^0$, $\eta' \rightarrow \pi^+\pi^-\eta$, and $\eta' \rightarrow \rho^0\gamma$ are assigned as individual systematic uncertainties.

The QC effect on the measured BFs has been corrected by the factor f_{QC} aforementioned and the residual error of f_{QC} is assigned as the systematic uncertainty, which is 0.7%.

The uncertainties arising from the finite sizes of the signal MC samples are (0.3 – 0.6)%. Systematic uncertainties from other selection criteria are found to be negligible.

For each signal decay, the total systematic uncertainty is obtained by summing individual contributions in quadrature and is shown in Table 2.

The BFs of D and \bar{D} decays, $\mathcal{B}_{\text{sig}}^+$ and $\mathcal{B}_{\text{sig}}^-$, are also measured separately. Their asymmetry is determined by $\mathcal{A}_{CP}^{\text{sig}} = \frac{\mathcal{B}_{\text{sig}}^+ - \mathcal{B}_{\text{sig}}^-}{\mathcal{B}_{\text{sig}}^+ + \mathcal{B}_{\text{sig}}^-}$. The obtained BFs and asymmetries are summarized in Table 3. No significant CP violation is observed. Several systematic uncertainties cancel in the asymmetry, such as the tracking and PID of $\pi^+\pi^-$, K^+K^- pairs, π^0, η reconstruction, quoted BFs, $K_S^0, \omega, \eta^{(\prime)}, \phi$ sideband choices, and the strong phase between D^0 and \bar{D}^0 decays. The other systematic uncertainties are estimated separately as above.

In summary, by analyzing 2.93 fb^{-1} of e^+e^- annihilation data taken at $\sqrt{s} = 3.773$ GeV with the BESIII detector, we have performed the first measurements of the absolute BFs of $D^0 \rightarrow K_L^0 \phi$, $D^0 \rightarrow K_L^0 \eta$,

$D^0 \rightarrow K_L^0 \omega$, and $D^0 \rightarrow K_L^0 \eta'$. Combining the BFs measured in this work with the known values for $\mathcal{B}(D^0 \rightarrow K_S^0 X)$ [1], the asymmetries of $\mathcal{B}(D^0 \rightarrow K_S^0 X)$ and $\mathcal{B}(D^0 \rightarrow K_L^0 X)$ are determined. Table 4 shows the comparison of the measured BFs and K_S^0 - K_L^0 asymmetries with the theoretical calculations of Ref. [6]. Clear asymmetries are found in $D^0 \rightarrow K_L^0 \eta, K_L^0 \eta'$, but none is found in the other two modes. Our results $\mathcal{R}(D^0, \eta) = 0.080 \pm 0.022$ and $\mathcal{R}(D^0, \eta') = 0.080 \pm 0.023$ are consistent with $\mathcal{R}(D^0, \pi^0) = 0.108 \pm 0.035$ measured by CLEO [10] and imply that the K_S^0 - K_L^0 asymmetry in $D^0 \rightarrow K_{S/L}^0 \eta, K_{S/L}^0 \eta'$ modes is approximately $2 \tan^2 \theta_C$ as expected based on SU(3) symmetry [2–6]. Comparing with the $\mathcal{R}(D^+, \pi^+)$ [10] and $\mathcal{R}(D_s^+, K^+)$ [48], a significantly larger asymmetry for $\mathcal{R}(D^0, X)$ is expected due to a smaller strong phase difference between the DCS and CF amplitudes. However, the obtained K_S^0 - K_L^0 asymmetries in $D^0 \rightarrow K_{S,L}^0 \phi$ and $K_{S,L}^0 \omega$ decays disagree with the predicted value [6] by 2.4σ and 4.4σ , respectively. The main possible reason of this tension is that the $E_P = E_V$ assumption in Ref. [6] is not satisfied. In addition, the asymmetries of the CP -conjugate BFs for these D decays are determined and no significant CP violation is found. These results offer crucial information to more reliably calculate the BFs of the $D \rightarrow PP$ and $D \rightarrow VP$ decays in theories and will aid investigations of quark SU(3)-flavor symmetry breaking as well as CP violation in the hadronic decays of charmed mesons [49, 50]. Our K_S^0 - K_L^0 asymmetries offer the first opportunity to access individual amplitudes of DCS processes involving K^0 which can be only measured with quantum correlated $e^+e^- \rightarrow D\bar{D}$ production near the threshold, thereby further restricting the $D^0 - \bar{D}^0$ mixing effect in charm decays.

The BESIII collaboration thanks the staff of BEPCII and the IHEP computing center for their strong support. This work is supported in part by the National Key R&D Program of China under Grants Nos. 2020YFA0406400 and No. 2020YFA0406300; the National Natural Science Foundation of China (NSFC) under Grants No. 11775230, No. 12035009, No. 11875170, No. 11475090, No. 11625523, No. 11635010, No. 11735014, No.

Table 2. Systematic uncertainties (%) in the measurements of the BF's.

Source	$K_L^0 \phi_{K^+K^-}$	$K_L^0 \eta_{\gamma\gamma}$	$K_L^0 \eta_{\pi^+\pi^-\pi^0}$	$K_L^0 \omega_{\pi^+\pi^-\pi^0}$	$K_L^0 \eta'_{\pi^+\pi^-\eta}$	$K_L^0 \eta'_{\rho^0\gamma}$
ST yield N_{tag}	0.5	0.5	0.5	0.5	0.5	0.5
K^\pm/π^\pm tracking	0.4	-	0.3	0.2	0.6	0.2
K^\pm/π^\pm PID	0.3	-	0.2	0.2	0.2	0.2
γ reconstruction	-	-	-	-	-	1.0
π^0/η reconstruction	-	0.5	0.7	0.7	0.7	-
Mass window requirement	0.2	-	0.2	0.1	0.5	0.1
$N_{\text{charged}}^{\text{extra}}/\pi^0/\eta$	0.8	0.8	0.8	0.8	0.8	0.8
MM ² fit	0.9	2.3	2.4	1.1	1.4	1.2
Opening angle	1.4	1.4	1.4	1.3	0.9	1.6
Quoted BF's	1.0	0.5	1.2	0.7	1.2	1.3
MC statistics	0.6	0.3	0.5	0.5	0.6	0.4
Strong phase	0.7	0.7	0.7	0.7	0.7	0.7
Total	2.4	3.0	3.4	2.4	2.6	2.9

Table 3. CP -conjugate BF's ($\mathcal{B}_{\text{sig}}^+$ and $\mathcal{B}_{\text{sig}}^-$) and their asymmetries ($\mathcal{A}_{CP}^{\text{sig}}$). The first and second uncertainties are statistical and systematic, respectively.

Decay	$\mathcal{B}_{\text{sig}}^+$ (%)	$\mathcal{B}_{\text{sig}}^-$ (%)	$\mathcal{A}_{CP}^{\text{sig}}$ (%)
$D^0 \rightarrow K_L^0 \phi$	0.428 ± 0.029	0.405 ± 0.034	$2.7 \pm 5.4 \pm 0.7$
$D^0 \rightarrow K_L^0 \eta$	0.445 ± 0.018	0.421 ± 0.017	$2.8 \pm 2.9 \pm 0.4$
$D^0 \rightarrow K_L^0 \omega$	1.200 ± 0.030	1.121 ± 0.031	$3.4 \pm 1.9 \pm 0.6$
$D^0 \rightarrow K_L^0 \eta'$	0.789 ± 0.028	0.826 ± 0.028	$-2.2 \pm 2.5 \pm 0.4$

11822506, No. 11835012, No. 11935015, No. 11935016, No. 11935018, No. 11961141012, No. 12022510, No. 12025502, No. 12035013, No. 12061131003, No. 12192260, No. 12192261, No. 12192262, No. 12192263, No. 12192264, and No. 12192265; the Chinese Academy of Sciences (CAS) Large-Scale Scientific Facility Program; Joint Large-Scale Scientific Facility Funds of the NSFC and CAS under Grants No. U1732263 and No. U1832207; CAS Key Research Program of Frontier Sciences under Grant No. QYZDJ-SSW-SLH040; 100 Talents Program of CAS; INPAC and Shanghai Key Laboratory for Particle Physics and Cosmology; ERC under Grant No. 758462; European Union Horizon 2020 research and innovation programme under Marie Skłodowska-Curie Grant Agreement No. 894790; German Research Foundation DFG under Grant No. 443159800, Collaborative Research Center CRC 1044, FOR 2359, GRK 214; Istituto Nazionale di Fisica Nucleare, Italy; Ministry of Development of Turkey under Grant No. DPT2006K-120470; National Science and Technology fund; Olle Engkvist Foundation under Grant No. 200-0605; STFC (United Kingdom); The Knut and Alice Wallenberg Foundation (Sweden) under Grant No. 2016.0157; The Royal Society, UK under Grants No.

DH140054 and No. DH160214; The Swedish Research Council; and U. S. Department of Energy under Awards No. DE-FG02-05ER41374 and DE-SC-0012069.

- [1] P. A. Zyla *et al.* (Particle Data Group), *Prog. Theor. Exp. Phys.* **2020**, 083C01 (2020).
- [2] I. I. Bigi and H. Yamamoto, *Phys. Lett. B* **349**, 363 (1995).
- [3] J. L. Rosner, *Phys. Rev. D* **74**, 057502 (2006).
- [4] B. Bhattacharya and J. L. Rosner, *Phys. Rev. D* **81**, 014026 (2010).
- [5] D. N. Gao, *Phys. Rev. D* **91**, 014019 (2015).
- [6] D. Wang, F. S. Yu, P. F. Guo, and H. Y. Jiang, *Phys. Rev. D* **95**, 073007 (2017).
- [7] D. Wang, F. S. Yu, and H. N. Li, *Phys. Rev. Lett.* **119**, 181802 (2017).
- [8] Y. Amhis *et al.* (HFLAV), *Eur. Phys. J. C* **77**, 895 (2017).
- [9] D. N. Gao, *Phys. Lett. B* **645**, 59 (2007).
- [10] Q. He *et al.* (CLEO Collaboration), *Phys. Rev. Lett.* **100**, 091801 (2008).
- [11] R. L. Kingsley, S. B. Treiman, F. Wilczek and A. Zee, *Phys. Rev. D* **11**, 1919 (1975).
- [12] M. Gronau, *Phys. Lett. B* **730**, 221 (2014); Erratum: *Phys. Lett. B* **735**, 282 (2014).
- [13] H. J. Lipkin, *Phys. Rev. Lett.* **46**, 1307 (1981).
- [14] H. Y. Cheng and C. W. Chiang, *Phys. Rev. D* **81**, 074021 (2010).
- [15] Q. Qin, H. N. Li, C. D. Lü, and F. S. Yu, *Phys. Rev. D* **89**, 054006 (2014).
- [16] H. Y. Cheng, C. W. Chiang, and A. L. Kuo, *Phys. Rev. D* **93**, 114010 (2016).
- [17] W. Kwong and S. P. Rosen, *Phys. Lett. B* **298**, 413 (1993).
- [18] Y. Grossman and D. J. Robinson, *J. High Energy Phys.* **04**, 067 (2013).
- [19] H. N. Li, C. D. Lü, and F. S. Yu, *Phys. Rev. D* **86**, 036012 (2012).

Table 4. Comparison of measured BF's and K_S^0 - K_L^0 asymmetries with theoretical calculations of Ref. [6]. \mathcal{B}_{exp} (\mathcal{B}_{FAT}) and $\mathcal{R}(D^0)_{\text{exp}}$ ($\mathcal{R}(D^0)_{\text{FAT}}$) are the BF's and K_S^0 - K_L^0 asymmetries of the experimental measurements (theoretical calculations).

Decay	\mathcal{B}_{exp} (%)	\mathcal{B}_{FAT} (%)	Difference	$\mathcal{R}(D^0)_{\text{exp}}$	$\mathcal{B}(D^0)_{\text{FAT}}$	Difference
$D^0 \rightarrow K_L^0 \phi$	$0.414 \pm 0.021 \pm 0.010$	0.33 ± 0.03	2.2σ	-0.001 ± 0.047	0.113 ± 0.001	2.4σ
$D^0 \rightarrow K_L^0 \eta$	$0.433 \pm 0.012 \pm 0.010$	0.40 ± 0.07	0.5σ	0.080 ± 0.022		1.5σ
$D^0 \rightarrow K_L^0 \omega$	$1.164 \pm 0.022 \pm 0.028$	0.95 ± 0.15	1.4σ	-0.024 ± 0.031		4.4σ
$D^0 \rightarrow K_L^0 \eta'$	$0.809 \pm 0.020 \pm 0.016$	0.77 ± 0.07	0.5σ	0.080 ± 0.023		1.6σ

- [20] Q. Qin, C. Wang, D. Wang, S. H. Zhou, [arXiv:2111.14472\[hep-ph\]](https://arxiv.org/abs/2111.14472).
- [21] Z. Z. Xing, *Mod. Phys. Lett. A* **34**, 1950238 (2019).
- [22] M. Ablikim *et al.* (BESIII Collaboration), *Phys. Rev. Lett.* **124**, 241802 (2020).
- [23] M. Ablikim *et al.* (BESIII Collaboration), *J. High Energy Phys.* **05**, 164 (2021).
- [24] I. I. Bigi, A. Paul, and S. Recksiegel, *J. High Energy Phys.* **06**, 089 (2011).
- [25] G. Isidori, J. F. Kamenik, Z. Ligeti, and G. Perez, *Phys. Lett. B* **711**, 46 (2012).
- [26] J. Brod, A. L. Kagan, and J. Zupan, *Phys. Rev. D* **86**, 014023 (2012).
- [27] H. Y. Cheng and C. W. Chiang, *Phys. Rev. D* **86**, 014014 (2012).
- [28] H. Y. Cheng and C. W. Chiang, *Phys. Rev. D* **100**, 093002 (2019).
- [29] H. N. Li, C. D. Lü, and F. S. Yu, [arXiv:1903.10638\[hep-ph\]](https://arxiv.org/abs/1903.10638).
- [30] R. Aaij *et al.* (LHCb Collaboration), *Phys. Rev. Lett.* **122**, 211803 (2019).
- [31] M. Ablikim *et al.* (BESIII Collaboration), *Chin. Phys. C* **37**, 123001 (2013); *Phys. Lett. B* **753**, 629 (2016).
- [32] M. Ablikim *et al.* (BESIII Collaboration), *Nucl. Instr. Method A* **614**, 345 (2010).
- [33] S. Agostinelli *et al.* (GEANT4 Collaboration), *Nucl. Instr. Method A* **506**, 250 (2003).
- [34] S. Jadach, B. F. L. Ward, and Z. Was, *Phys. Rev. D* **63**, 113009 (2001); *Comput. Phys. Commun.* **130**, 260 (2000).
- [35] D. J. Lange, *Nucl. Instrum. Meth. A* **462**, 152 (2001); R. G. Ping, *Chin. Phys. C* **32**, 599 (2008).
- [36] J. C. Chen, G. S. Huang, X. R. Qi, D. H. Zhang, and Y. S. Zhu, *Phys. Rev. D* **62**, 034003 (2000); R. L. Yang, R. G. Ping and H. Chen, *Chin. Phys. Lett.* **31**, 061301 (2014).
- [37] E. Richter-Was, *Phys. Lett. B* **303**, 163 (1993).
- [38] R. M. Baltrusaitis *et al.* (MARKIII Collaboration), *Phys. Rev. Lett.* **56**, 2140 (1986).
- [39] M. Ablikim *et al.* (BESIII Collaboration), *Phys. Rev. Lett.* **124**, 241803 (2020).
- [40] M. Ablikim *et al.* (BESIII Collaboration), *Phys. Lett. B* **734**, 227 (2014).
- [41] H. Albrecht *et al.* (ARGUS Collaboration), *Phys. Lett. B* **241**, 278 (1990).
- [42] M. Ablikim *et al.* (BESIII Collaboration), *Phys. Rev. D* **100**, 072006 (2019).
- [43] T. Evans, S. T. Harnew, J. Libby, S. Malde, J. Rademacker, and G. Wilkinson, *Phys. Lett. B* **757**, 520 (2016).
- [44] Heavy Flavor Averaging Group (HFLAV), <https://hflav.web.cern.ch/content/charm-physics>
- [45] M. Ablikim *et al.* (BESIII Collaboration), *Eur. Phys. J. C* **76**, 369 (2016).
- [46] M. Ablikim *et al.* (BESIII Collaboration), *Phys. Rev. D* **97**, 072004 (2018).
- [47] M. Ablikim *et al.* (BESIII Collaboration), *Phys. Rev. D* **86**, 052011 (2012).
- [48] M. Ablikim *et al.* (BESIII Collaboration), *Phys. Rev. D* **99**, 112005 (2019).
- [49] M. Ablikim *et al.* (BESIII Collaboration), *Chin. Phys. C* **44**, 040001 (2020).
- [50] H. B. Li and X. R. Lyu, *Natl. Sci. Rev.* **8**, nwab181 (2021).